Geochimica et Cosmochimica Acta 367 (2024) 123–132

Contents lists available at ScienceDirect

Geochimica et Cosmochimica Acta

journal homepage: www.elsevier.com/locate/gca

Stable isotope composition and concentration systematics of Ca and trace elements (Zn, Sr) in single aliquots of fossil bone and enamel

Danaé Guiserix [a,1], Pierre-Jean Dodat [a,1], Klervia Jaouen [b], Emmanuelle Albalat [a], Jessica Mendes Cardoso [b], Bruno Maureille [c], Vincent Balter [a,*]

[a] LGL-TPE, Ecole Normale supérieure de Lyon, UMR 5276, CNRS, 69342 Lyon Cedex 07, France
[b] GET, Observatoire Midi Pyrénées, UMR 5563, CNRS, 31400 Toulouse, France
[c] PACEA, Univ. Bordeaux, UMR 5199, CNRS, Ministère de la Culture, F-33600 Pessac, France

ARTICLE INFO

Associate editor: Daniel Sinclair

Keywords:
Non-traditional stable isotopes
Calcium
Zinc
Strontium
Trophic chain
Fossil bone
Fossil enamel

ABSTRACT

Measurements of modern bone and tooth enamel show that calcium stable isotopes ($\delta^{44}Ca$), zinc ($\delta^{66}Zn$), and strontium ($\delta^{88}Sr$) have great potential as ecological and dietary tracers for studies on fossil material. Despite the fact that these three elements can be recovered using sequential chromatographic extraction from a single aliquot, a multi-proxy study has not been attempted yet, which would allow a less destructive analysis of precious fossil material. The present study consists of analyzing $\delta^{44}Ca$, $\delta^{66}Zn$, $\delta^{88}Sr$, and $^{87}Sr/^{86}Sr$ values in fossil bone and tooth enamel of carnivore and herbivore mammals from the Camiac cave (Upper Pleistocene, Gironde, France). Our study aims at (1) developing a protocol for Ca, Zn, and Sr stable isotope analyses from a single fossil bone or enamel aliquot; (2) testing the respective preservation of biological isotopic signatures in bone and tooth enamel; and (3) comparing the patterning of the different isotopic systems in a fossil mammal community. In the present study, fossil enamel samples have not been leached, as it has been done so far for Zn isotope analyses, but fossil bone samples have been leached using diluted acetic acid or were left unleached. Using inclusive statistical analyses, we identify the effect of leaching on bone chemical compositions, and the concentration and isotope composition of Ca, Zn, and Sr in leached bone and unleached enamel show no sizeable diagenetic overprint. We report for the first time $\delta^{66}Zn$ values in fossil bone. The results show that bone $\delta^{66}Zn$ values mirror the pattern already observed in enamel, e.g., a significant trophic ^{66}Zn depletion between herbivores and carnivores. Bone $\delta^{44}Ca$ and $\delta^{88}Sr$ values also mirror those in enamel, and the results highlight a clear distinction between ruminants and non-ruminants, the latter being ^{44}Ca-enriched. The present study focuses on the importance of analyzing several isotopic systems in a single fossil bone or enamel aliquot and shows encouraging results for the preservation of biological isotopic signatures in fossil bone, despite the longstanding dread of a so-called associated pervasive diagenesis. The present study will therefore be useful to consider any precious fossil material with limited destructive sampling possibilities.

1. Introduction

Many tools have been developed to decipher ancient diets, some of them originating more than 40 years ago from isotope geochemistry (e.g., Deniro and Epstein, 1981; DeNiro and Epstein, 1978). Recent studies on non-traditional stable isotopes have led to the development of new dietary proxies, for instance, Ca (e.g., Skulan and DePaolo, 1999), Zn (e.g., Jaouen et al., 2013), and Sr (e.g., Knudson et al., 2010). Even though these new paleodietary proxies look promising, more research needs to be done to find out what they can and cannot do. In particular, three possible problems need to be looked at: dietary and physiological systematics, sample destruction, and diagenesis.

Calcium is a bio-essential major element for vertebrates because it constitutes the main cation (~40 wt%) of carbonated hydroxylapatite (HAP), the mineral phase of bone, dentine, and enamel. Skulan and collaborators (Skulan et al., 1997) first described a linear correlation between the Ca isotope composition of diet and tissues, including bone. These observations allowed for a decrease in the Ca isotope composition

* Corresponding author.
E-mail address: vincent.balter@ens-lyon.fr (V. Balter).
[1] These authors contributed equally.

https://doi.org/10.1016/j.gca.2023.12.021
Received 4 August 2023; Accepted 15 December 2023
Available online 18 December 2023

($\delta^{44}Ca$) up a marine trophic chain (Skulan and DePaolo, 1999). Several authors further assessed the extent of this offset using different animal models, resulting in an average difference of the $\delta^{44}Ca$ values between bone and diet of ca. −0.6 ‰ (Skulan and DePaolo, 1999; Tacail et al., 2020) and an average difference of ca. −0.3 ‰ of the $\delta^{44}Ca$ values between bone of prey and predator (Martin et al., 2018). At first glance, Ca isotopes are thus a relevant paleodietary proxy (Martin et al., 2017a), but evaluating the proportion of consumed meat versus plants is not possible because the $\delta^{44}Ca$ values of both components are similar (Tacail et al., 2017). Bone consumption has been proposed to explain the observed decrease of the $\delta^{44}Ca$ values up trophic chains, which could explain the Ca isotope systematics in terrestrial (Heuser et al., 2011; Hassler et al., 2018; Hu et al., 2022) or marine (Clementz et al., 2003; Martin et al., 2017b) and more recently in hominins (Tacail et al., 2017; Martin et al., 2020; Dodat et al., 2021; Hu et al., 2022). In high-resolution mode on multi-collector inductively coupled plasma mass spectrometry (MC-ICPMS), Ca stable isotope compositions are measured at 1–2 mg/L, and because Ca is stochiometric in HAP, a sample amount of 5 µg of bone or enamel is theoretically sufficient. However, such a minuscule amount of material cannot be manipulated easily, so a minimum of ca. 100 µg is classically collected, which can be achieved using a micro-drill device (Tacail et al., 2017). Calcium stable isotope compositions in enamel can also be analyzed using laser ablation (LA-MC-ICPMS), a quasi-non-destructive approach since teeth are already cut (Tacail et al., 2015). As a consequence of the abundance of Ca in HAP, Ca isotopes are quite resistant to diagenesis, even probably immune to diagenesis in enamel because the porosity is so low that it cannot account for enough Ca-bearing secondary minerals to modify the bulk Ca isotope composition (Dodat et al., 2023).

Radiogenic strontium ratio ($^{87}Sr/^{86}Sr$) is a longstanding tool in forensics, ecology, bioarcheology, and paleoanthropology to study present and past migrations and landscape use (Müller et al., 2003; Lazzerini et al., 2021; Wooller et al., 2021). To correct for natural fractionation and instrumental mass bias, the measurement of the $^{87}Sr/^{86}Sr$ ratio is normalized using a constant $^{88}Sr/^{86}Sr$ stable isotope ratio. Thanks to the development of MC-ICPMS in the last twenty years, it is now possible to measure simultaneously the radiogenic $^{87}Sr/^{86}Sr$ and stable ($\delta^{88}Sr$) Sr isotope ratios, allowing mobility and diet interpretations (Knudson et al., 2010; Lewis et al., 2017; Guiserix et al., 2022). These latter are based on the fact that Sr is not a bio-essential element, but because of its similar atomic properties to Ca, Sr is incorporated into the body as a Ca substitute where it undergoes discrimination processes known as calcium biopurification (Balter, 2004). It is thus anticipated that the Sr isotope systematics will resemble that of Ca, an assumption that is supported by a previous study in a freshwater invertebrate community (Nitzsche et al., 2022). Laser ablation is widely used to analyze radiogenic Sr (Fietzke et al., 2008; Balter et al., 2008; Lazzerini et al., 2021), but as a trace element, Sr concentration is too low in enamel (few tenths of mg/g) to allow the measurement of the $\delta^{88}Sr$ value using LA-MC-ICPMS. Between 3 and 10 mg of bone or tooth enamel is required to measure the $\delta^{88}Sr$ value, whose sensitivity to diagenesis can be significant depending on the taphonomic context (Budd et al., 2000; Reynard and Balter, 2014; Nava et al., 2020).

Zinc is a bio-essential trace element, and the Zn stable isotope composition ($\delta^{66}Zn$) in enamel has been studied in both modern (Jaouen et al., 2013, 2016a, 2016b) and fossil (Bourgon et al., 2020, 2021; McCormack et al., 2021, 2022) material. The trophic properties of the Zn isotope composition are based on the different $\delta^{66}Zn$ values of plant products and muscle, with plant products usually having the most elevated $\delta^{66}Zn$ values (Jaouen et al., 2013, 2016a), whereas muscles exhibit lower values (Balter et al., 2010, 2013). As a result, the $\delta^{66}Zn$ value decreases by 0.3 ‰ to 0.6 ‰ from modern herbivores to carnivores (Jaouen et al., 2013, 2016a, 2016b; Bourgon et al., 2020, 2021). Previous studies have shown that the original trophic signature is preserved in fossil tooth enamel (Bourgon et al., 2020; McCormack et al., 2021) however, no investigations on fossil bone have been performed yet. The Zn concentration is comparable to that of Sr both in bone and enamel thus, the measurement of both isotope compositions is likely from a single aliquot, the measurement of the $\delta^{66}Zn$ value using LA-MC-ICPMS is currently impossible and the sensitivity of Zn to diagenesis can also be significant in fossil bone (Weber et al., 2021).

By analyzing the $\delta^{44}Ca$, $\delta^{66}Zn$, $\delta^{88}Sr$, and $^{87}Sr/^{86}Sr$ values in bone (n = 29) and enamel (n = 26) coming from a unique fossil assemblage (Camiac, Upper Pleistocene, Gironde, France), the objectives of the present study are threefold. The first objective is to setup an ion-exchange chromatography protocol allowing the isolation and purification of Ca, Zn, and Sr from HAP for stable isotope analyses. The second objective is to assess the extent of diagenesis of Ca, Zn, and Sr isotope compositions in unleached fossil enamel and in leached and unleached fossil bone. The third objective is to investigate the Ca, Zn, and Sr isotope systematics in bone and enamel at the species level. For the first objective, we developed an ion-exchange chromatography in which Ca and Sr were isolated and purified at Laboratoire de Géologie de Lyon: Terre Planètes Environnement (LGL-TPE), and Zn was isolated and purified at Géosciences Environnement Toulouse (GET). To achieve the second objective, we proceeded to multiple regression analyses using the set of isotope compositions and trace element concentrations to highlight potential correlations between Ca, Zn, and Sr isotope compositions and concentrations on the one hand, and trace element concentrations known to be of diagenetic origin on the other hand. Isolated bone and tooth vestiges were collected for two different omnivore and carnivore taxa and a large group of herbivore taxa with various dietary preferences to conduct the third objective dedicated to studying the bone vs. enamel Ca, Zn, and Sr isotope systematics at the species level.

2. Material

The fossil material was found in the Camiac cave (Gironde, France), excavated in 1974 by Lenoir (2000). The site is a cave hyena den from the Late Mousterian period, considering the lithic collection and the single collagen ^{14}C datation (Guadelli, 1989). The fossil materials found in this cave had already been the subject of several taphonomic and morphologic studies (Discamps, 2011; Discamps et al., 2012). Three ungulates, the horse, bovine, and woolly rhinoceros, for whom bones are found to have gnawing traces by hyenas, dominate this assemblage (Guadelli, 1989; Discamps, 2011). The faunal assemblage thus includes cave hyena (*Crocuta spelaea*), but also cave lion (*Panthera spelaea*), cave bear (*Ursus spelaeus*), boar (*Sus scrofa*), red deer (*Cervus elaphus*), megaloceros (*Megaloceros giganteus*), woolly rhinoceros (*Coelodonta antiquitatis*), woolly mammoth (*Mammuthus primigenius*), bison or auroch (*Bison* sp.), and horse (*Equus caballus*). Bone samples have been stored at LGL-TPE in powder since 2002 (Balter et al., 2002a,b). A new sampling was performed for enamel, for which only late-forming teeth (2nd and 3rd molars) were selected to avoid any suckling effects. The list of fossil materials is given in Supplementary Material.

Certified reference materials (CRMs) were used for a quality control assessment of the concentrations and isotope compositions. The bone ash “SRM-1400” and bone meal “SRM-1486” provided by the National Institute of Standards and Technology (NIST) were analyzed in the course of the study both at LGL-TPE and GET. The effect of leaching was also investigated on these CRMs. The list of CRMs is given in Supplementary Material.

3. Methods

3.1. Sampling, leaching, and digestion protocols

The surface of the fossil tooth enamel was cleaned with an abrasive drill bit and then sampled by drilling using a bit diameter of 0.8 mm. Regarding bone, when the amount of collected sample was enough, it was split for leaching or direct dissolution. Regarding enamel, the amount of sample collected was always insufficient to perform a

leaching step.

The principle of the leaching procedure is to remove secondary Ca-bearing carbonates ($CaCO_3$) that may have precipitated during diagenesis, thanks to the higher dissolution coefficient of $CaCO_3$ compared to HAP. However, the leaching itself can generate artificial isotope fractionation with a potential preferential leaching of light isotopes. To test this hypothesis, we performed the leaching procedure on CRMs. The leaching protocol used in this study was inspired by that described by Balter et al. (2001, 2002a,b), i.e., the sample was soaked in 10 mL of ultrapure 0.1 M acetic acid (Seastar Chemicals) and ultrasonicated for 30 min. The sample was then centrifuged for 5 min at 5000 rpm, with the supernatant withdrawn and replaced by 10 mL of 18.2 MΩ.cm-grade MilliQ water. The rinsing procedure was repeated three times, then the sample was dried down overnight at 90 °C and transferred into Savillex PFA beakers for acid digestion, which was performed using distilled concentrated HNO_3. In many instances, the amount of remaining material was so small that weighting was not performed. For the samples that were weighed before and after the leaching, the procedure resulted in a loss of 57 % (±23 %; ±2 SD; n = 26) of the initial mass. The results of concentration are thus expressed using Ca normalization.

3.2. Ca, Zn, and Sr purification protocols

For stable isotope analysis of Ca, Sr, and Zn, the elements of interest must be chemically separated from the matrix so that there are no interfering elements present when the measurements are made with MC-ICPMS. Ion-exchange column chromatography is used to separate Ca, Sr, and Zn from a single aliquot, following a protocol that is fully explained in Table S1. The first step was processed according to le Goff et al. (2021) to separate Ca + Sr and Zn from the matrix. The Sr purification step followed the protocol of Guiserix et al. (2022), the Ca purification step was slightly modified from Tacail et al. (2014) for small aliquots, and the Zn purification step was processed according to Moynier et al. (2006). This overall protocol was applied to the entire set of enamel samples. However, some of the bone samples included in the present study were already analyzed for Ca isotope composition (Dodat et al., 2023). For these samples, we did not separate Ca to measure the δ^{44}Ca value again. Instead, Sr and Zn were separated at GET using the same aliquot that was used for Ca isotope analyses. It must be noted that before the Zn separation step, there is a risk of mixing between nitrates (coming from the HNO_3 3 N) and HBr, which can form Br_2 (an orange gas). The coloration of the solution when adding HBr to the dry sample indicates an excess of remaining nitrates that could interact with the AG1X8 resin, leading to an early elution of Zn along with a procedural isotope fractionation favoring light isotopes. We observed such an orange coloration in the GET ID "SRM-1400b" sample (Supplementary Material). The resulting δ^{66}Zn value of 1.16 ‰ is shifted from the referenced value by ~0.2 ‰. Other aliquots of the SRM-1400 CRM did not present this coloration and had a δ^{66}Zn value very close to the expected value of 0.96 ± 0.08 ‰ (Jaouen et al., 2020). To prevent the formation of Br_2, we suggest drying the sample after the Sr separation, adding 1 mL of distilled concentrated HCl, and then evaporating before retaking in HBr for Zn separation. This step may be processed twice.

3.3. Concentration measurements

The concentration of major elements (Mg, P, and Ca) was determined on an inductively coupled plasma optical emission spectrometer (ICP-OES, iCAP Pro Series, Thermo Scientific) at LGL-TPE. The concentration of minor elements (Mg, Al, S, Ti, V, Mn, Fe, Cu, Zn, Sr, Ba, and U) was determined by ICPMS (iCap-Q, Thermo Scientific) at LGL-TPE and at GET (iCap-TQ, Thermo Scientific). Aliquots of 20 µL were taken from digested samples and diluted in 0.5 N HNO_3 with In, Sc, or Rh as internal standards. Procedural Sr blanks were between 0.5 and 1.5 ng, which was typically 0.03 % of total Sr, Zn blanks were between 5 and 15 µg which was typically 0.5 % of total Zn, and Ca blanks were under the limit of quantification by ICP-OES. Because concentrations were calculated with two dilutions (one on ICPMS for trace elements and the second on ICP-OES for Ca), we calculated the trace element Ca-normalized ratios by concatenating its Mg-normalized ratio and the Ca/Mg ratio (Balter and Lécuyer, 2004).

3.4. Isotope composition measurements

The measurements of isotope compositions were performed by MC-ICPMS for Ca (Thermo Neptune Plus, Thermo Scientific) at LGL-TPE, for Zn (Thermo Neptune Plus, Thermo Scientific) at GET, and for Sr (Nu Plasma 500, Nu Instrument) at LGL-TPE.

The Ca isotope compositions were measured using the protocol and cup configuration described by Tacail et al. (2014), with a sample-standard bracketing procedure. The in-house ICP-Ca_{Lyon} standard was used as the bracketing standard, and variations of the $^{44}Ca/^{42}Ca$ ratio in samples relative to this standard are expressed in δnotation, defined as:

$$\delta^{44}Ca_{ICP-Ca\ Lyon} = \left[\frac{(^{44}Ca/^{42}Ca)_{sample}}{(^{44}Ca/^{42}Ca)_{ICP-Ca\ Lyon}} - 1\right] \times 1000$$

Variations of the $^{43}Ca/^{42}Ca$ ratio were also measured to monitor mass-dependence fractionation and reported as δ^{43}Ca values (Supplementary Material). The δ^{44}Ca values are reported relative to the SRM915a standard using a constant difference of −0.518 ± 0.025 ‰ (±2 SD).

The Zn isotope compositions were measured using the protocol and cup configuration described by Moynier et al. (2006) modified by Jaouen et al. (2016a), with Cu doping for external correction of mass bias and a sample-standard bracketing procedure. The in-house AA-MPI Zn standard was used as the bracketing standard, and variations of the $^{66}Zn/^{64}Zn$ ratio in samples relative to this standard are expressed in δnotation, defined as:

$$\delta^{66}Zn_{AA-MPI\ Zn} = \left[\frac{(^{66}Zn/^{64}Zn)_{sample}}{(^{66}Zn/^{64}Zn)_{AA-MPI\ Zn}} - 1\right] \times 1000$$

Variations of the $^{67}Zn/^{64}Zn$ and $^{68}Zn/^{64}Zn$ ratios were also measured to monitor mass-dependance fractionation and reported as δ^{67}Zn and δ^{68}Zn values, respectively (Supplementary Material). The δ^{66}Zn values are reported relative to the JMC-Lyon standard using a constant difference of 0.27 ‰.

The Sr isotope compositions were measured using the protocol and cup configuration described by Guiserix et al. (2022). A high-purity Zr solution (Alfa Aesar, 1000 ppm) was diluted and added to the standard and sample solutions at 450 µg/L to reach a $^{90}Zr/^{88}Sr$ ratio close to unity. Daily calibration was made to optimize operating conditions for maximum Sr and Zr signal stability, which was monitored with repeated measurements on the SRM-987 (NIST) standard solution, also used for the sample-standard bracketing procedure. The contribution of Kr coming with the Ar gas on ^{86}Sr was monitored by performing an on-peak baseline measurement on a 0.05 N HNO_3 solution. Variations of the $^{88}Sr/^{86}Sr$ ratio in samples relative to the SRM-987 standard are expressed in δ notation, defined as:

$$\delta^{88}Sr_{\ SRM-987} = \left[\frac{(^{88}Sr/^{86}Sr)_{sample}}{(^{88}Sr/^{86}Sr)_{SRM-987}} - 1\right] \times 1000$$

4. Results

4.1. Mass fractionation dependency

Plots of δ^{44}Ca vs. δ^{43}Ca (Fig. S1A), δ^{67}Zn vs. δ^{66}Zn (Fig. S1B), and δ^{68}Zn vs. δ^{66}Zn (Fig. S1C) yield the mass fractionation relationships in three-isotope spaces, allowing the calculation of slopes (β) of the respective best-fit linear regressions. The slope values are 1.970 ± 0.038

for $\delta^{43}Ca$ vs. $\delta^{42}Ca$, $\delta^{67}Zn$ vs. $\delta^{66}Zn$ for 1.484 ± 0.047, and 1.928 ± 0.026 for $\delta^{68}Zn$ vs. $\delta^{66}Zn$, which are in excellent agreement with theoretical β values calculated either with an equilibrium mass-dependent isotope fractionation (1.951, 1.479, and 1.942, respectively) or a kinetic mass-dependent isotope fractionation (1.974, 1.490, and 1.971, respectively; Young et al., 2002). Overall, we have thus considered as valid all measured isotopic data except the Zn isotope values measured for the CRM SRM-1400b (GET ID, Supplementary Material, see discussion above in Section 3.2).

4.2. Isotope compositions and concentrations of CRMs

The $\delta^{44}Ca$, $\delta^{66}Zn$, and $\delta^{88}Sr$ values have been analyzed in treated and untreated SRM-1400 and SRM-1486 CRMs to test the reliability of the protocol. The results, with numbers of replicates for each aliquot, are given in Supplementary Material. The expected isotopic values of SRM-1400 are calculated from literature references, with the average being −1.10 ± 0.17 ‰ (±2 SD; Koutamanis et al., 2021; Lanping et al., 2018; Romaniello et al., 2015; Tacail et al., 2014) for the $\delta^{44}Ca$ value, 0.96 ± 0.08 ‰ for the $\delta^{66}Zn$ value (±2 SD; Jaouen et al., 2020) and, −0.32 ± 0.02 ‰ for the $\delta^{88}Sr$ value (±2 SD; Brazier et al., 2019; Guiserix et al., 2022; Romaniello et al., 2015; Zimmermann et al., 2019). The measured isotopic values of SRM-1400 are −1.10 ± 0.12 ‰ (±2 SD, n = 5) for the $\delta^{44}Ca$ value, 0.86 ± 0.14 ‰ (±2 SD, n = 6) for the $\delta^{66}Zn$ value and −0.32 ± 0.06 ‰ (±2 SD, n = 7) for the $\delta^{88}Sr$ value (Supplementary Material). These are undistinguishable from the expected values, validating the reliability of the separation protocol and the measurement procedure. Of importance, the leaching has no sizeable effect on any of the isotope compositions of the CRMs (Fig. 1A–D; Supplementary Material), demonstrating that this pretreatment method does not induce a procedural isotopic fractionation.

The Ca-normalized ratios of trace element concentrations are shown in Fig. S2. Generally, the measured values show good agreement with the certified values, except for Al/Ca and Mg/Ca ratios, for which the measured values are moderately too low. Regarding the SRM-1486 CRM, the measured Mn/Ca and Fe/Ca ratios are slightly too high and the Sr/Ca ratio too low, respectively, compared to the certified values. As already highlighted for the isotopic compositions, the leaching step has no sizeable effect on the Ca-normalized concentration of trace elements.

The overall accuracy of the Ca, Zn, and Sr isotope composition and concentration of the CRMs suggests that our first objective, which was to setup an ion-exchange chromatography allowing the isolation and purification of Ca, Zn, and Sr from HAP for stable isotope analyses, is fulfilled.

4.3. Preservation indicators

4.3.1. Preservation of fossil bone

As mentioned above, the leaching step has no effect on the Ca, Zn, and Sr isotope compositions of CRMs (Supplementary Material), indicating that when the sample is only composed of HAP, the partial dissolution is quantitative and thus does not induce procedural isotope fractionation. The situation is, however, different in fossil bone, which also contains $CaCO_3$ with its attendant profile of diagenetic trace elements. For Ca, untreated fossil bone always displays higher Ca/P (Fig. S3A) and $\delta^{44}Ca$ (Fig. 1A) values compared to treated bone due to the pervasive presence of $CaCO_3$ in the porosity, which usually has a $\delta^{44}Ca$ close to 0 ‰ (Dodat et al., 2023). The difference between unleached and leached $\delta^{44}Ca$ values ($\Delta_{L}\text{-}\delta_{Ca}$) is significant (0.21 ± 0.10 ‰, ±2 SD) in fossil bone, which indicates that these is a compulsory *ad hoc* step to potentially recover biogenic $\delta^{44}Ca$ values. Regarding Zn, untreated bone always displays Zn/Ca ratios lower than treated bone ($\Delta_{L\text{-}Zn/Ca} = 4.10^{-4} \pm 3.10^{-4}$, ±2 SD; Fig. S3B), which is due to the removal of $CaCO_3$. However, there is no consistent difference between untreated and treated fossil bone $\delta^{66}Zn$ values (Fig. 1B), both being most generally similar, the $\Delta_{L}\delta_{Zn}$ value being 0.00 ± 0.11 ‰ (±2 SD) in fossil bone samples, respectively. This can be explained by the absence of a significant amount of diagenetic Zn present in the leached $CaCO_3$. Regarding Sr, there is no consistent difference between untreated and treated fossil bone Sr/Ca values, despite significant possible differences (for instance, D3-22 and B2-52, Fig. S3B). The stable $\delta^{88}Sr$ (Fig. 1C) and radiogenic $^{87}Sr/^{86}Sr$ (Fig. 1D) values between untreated and treated fossil bone are minimal ($\Delta_{L}\text{-}\delta_{Sr}$ = -0.02 ± 0.06 ‰ and $\Delta_{L\text{-}Sr/Sr} = 4.10^{-5} \pm 10^{-4}$, ±2 SD). The absence of any concentration or isotope composition systematics between untreated and treated bone suggests that diagenetic Sr may be present in a significant and varying amount in $CaCO_3$.

To gain insight into possible mixing between a diagenetic and a biogenic pool with distinct concentrations and isotope compositions, we studied the distribution of the Ca, Zn, and Sr isotope compositions vs. the inverse Ca, Zn, and Sr concentration. Indeed, various proportions of a diagenetic overprinting will result in a correlation between the concentration and the isotope composition along a mixing hyperbola, i.e., a straight line, if the inverse of the concentration is instead considered (Reynard and Balter, 2014). Results show that a possible, yet not significant, correlation can exist between Ca/Sr and radiogenic and stable Sr isotope compositions in untreated bone (Fig. S4C and S4D, respectively), suggesting a Sr diagenetic overprinting in untreated fossil bone at Camiac. No such correlation exists between Ca and Zn in untreated bone (Fig. S4A and S4B, respectively). In treated bone, none of the isotope compositions is correlated to concentration, suggesting the efficient removal of Sr diagenetic overprinting by the leaching protocol (Fig. S5A–D).

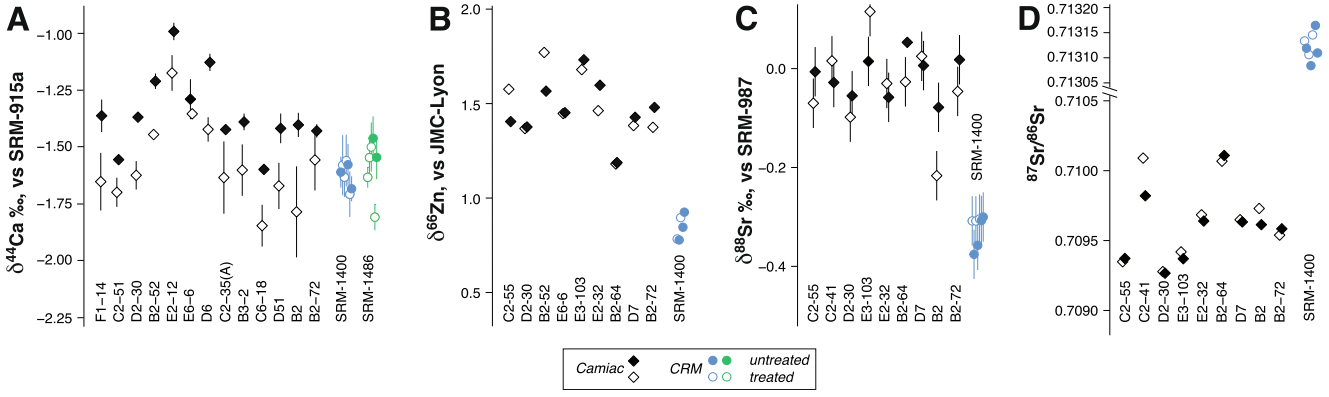

Fig. 1. Effect of leaching on fossil bone and CRMs isotope compositions. (A) Calcium isotope compositions ($\delta^{44}Ca$) of untreated and treated samples. Fossil bone data are from (Dodat et al., 2023). (B) Zinc isotope compositions ($\delta^{66}Zn$) of untreated and treated samples. (C) Strontium stable isotope compositions ($\delta^{88}Sr$) of untreated and treated samples. (D) Strontium radiogenic isotope compositions ($^{87}Sr/^{86}Sr$) of untreated and treated samples.

We next explore the effect of leaching on the whole composition of fossil bone using heatmaps of correlation coefficients between the set of concentrations and isotope compositions. We first construct such a heatmap for untreated fossil bone (Fig. S6A) and then generate the associated individual correlations with an adjusted p-value <0.05 (Fig. S7A) to check for the robustness of the statistics and to identify samples whose biogenic isotopic composition and/or concentration could be suspected to have been diagenetically perturbed. We therefore mainly focused on potential correlations between Ca, Zn, and Sr isotope compositions and Ca/P, Zn/Ca, and Sr/Ca ratios on the one hand and diagenetic Ca-normalized Al, Ti, V, Mn, Fe, and U concentrations on the other. Some elements (Mn, S, Ti, V and U) were not measured in unleached fossil bone, and inspection of Fig. S6A and S7A reveal that only the correlation of Al/Ca vs. Fe/Ca, characteristics of the presence of Fe- and Al-rich oxyhydroxides, is highly significant (p-value $< 10^{-7}$). Some possible other correlations, identifiable by the intense red or blue tones associated with a strong Pearson rho coefficient, are visible (Fig. S6A). However, these associations are withdrawn in leached fossil bone (Fig. S6B and S7B), while significant associations now appear between δ^{66}Zn and δ^{44}Ca or δ^{88}Sr. Interestingly, the Al/Ca vs. Fe/Ca correlation is still present in leached fossil bone, suggesting that the leaching procedure is inefficient at removing oxyhydroxides. No significant diagenetic effect on leached fossil bone has thus been detected using multi-dimensional correlations.

4.3.2. Preservation of fossil enamel

Enamel has not been leached, which can be an issue for trace element (e.g., Zn and Sr) isotope compositions. The heatmap of the correlation matrix shows that unleached fossil enamel has many significant relationships, but most of them are with diagenetic trace elements (Fig. S6C). While isotope compositions are not concerned, two significant correlations nevertheless retain attention, i.e., a first between Ca/P and V/Ca and a second between Mn/Ca and Zn/Ca (Fig. S6C). Inspection of the individual correlations reveals that three samples (B2-67, C2-51, and F1-34) and five samples (C2-51, C7-14, C7-17, E2-65, and E4-93) drive these positive correlations for Ca/P vs. V/Ca and Mn/Ca vs. Zn/Ca, respectively (Fig. S7C). While these correlations involve concentrations only, it seems that there is no influence of diagenetic V on the δ^{44}Ca values ($R = 0.12$, p-value $= 0.58$, Fig. S6C) or of diagenetic Mn on the δ^{66}Zn values ($R = 0.21$, p-value $= 0.30$, Fig. S6C). Further caution will, however, be taken with these samples.

Finally, we studied the distribution of the Ca, Zn, and Sr isotope compositions vs. the inverse Ca, Zn and Sr concentrations in untreated enamel and found no evidence of correlation (Fig. S8A–D), suggesting that all the studied isotope compositions in fossil enamel at Camiac are devoid of diagenetic overprinting.

5. Discussion

5.1. Preservation of biogenic stable and radiogenic isotope signatures

The Ca isotope composition in fossil enamel is probably immune to diagenesis because the enamel porosity cannot account for enough secondary $CaCO_3$ to modify the bulk HAP (Dodat et al., 2023). This probably holds because Ca is the major cation in HAP, constituting ca. 40 wt%, but is no longer the case for Zn and Sr, which are trace elements. In fossil bone, all the isotope compositions can be overprinted by diagenesis because the porosity is high enough to accommodate sufficient $CaCO_3$ and oxy-hydroxides to modify the biogenic values. Knowledge of the state of preservation of isotope compositions in the HAP of fossil bone and enamel is a difficult task as there is no absolute proxy for diagenesis. In this study, we use a combination of different *post-hoc* indicators, such as (1) the existence of a correlation between the isotope composition and the inverse of the concentration for a given element of ecological and/or physiological interest, and (2) the existence of a correlation between the isotope composition or the concentration for a given element of ecological and/or physiological interest with the concentration of an element known to be of diagenetic origin. At Camiac, the absence of any of these indicators in leached fossil bone supports the fact that the leaching protocol was successful for the recovery of Ca, Zn, and Sr isotope biogenic signatures in bone. The decrease in the Ca/P ratio (Fig. S3A) and the increase in the Zn/Ca ratio (Fig. S3B) between untreated and treated samples show that the leaching protocol effectively removes diagenetic Ca from fossil bone. The decrease of the Ca/P ratio during leaching is well described in the literature and is at the basis of the solubility profiles (Sillen and LeGeros, 1991), however, the increase of the Zn/Ca ratio during leaching of fossil bone is for the first time elucidated and could be used in further studies to scrutinize the preservation of Zn biogenic stable isotope composition. Of note, we do not observe any consistent variation regarding the Sr/Ca ratio during leaching, which agrees with the fact that $CaCO_3$ may contain a significant and varying amount of diagenetic Sr (Sillen and LeGeros, 1991). The absence of any of the above-mentioned indicators in unleached fossil enamel supports the fact that leaching was unnecessary, which is fortunately for considering that the isotope compositions of Zn and Sr, which are trace elements, are not significantly overprinted by diagenesis at Camiac. The results of this study only apply to the Camiac bone and enamel material. They cannot be transposed a priori to other fossil materials without assessing the above-mentioned *post-hoc* indicators of diagenesis. This is even more the case for older or more badly preserved fossil bone, which can contain in the HAP structure exogenous Ca, Sr, and Zn (and any other elements) coming from recrystallized $CaCO_3$.

5.2. Sr/Ca and Ba/Ca systematics

The trace element Sr/Ca and Ba/Ca ratios were already measured in some bone samples and reported in Balter et al. (2002a). However, the present results only compare moderately with this previous study, with 4 samples out of 24 being offset for the Sr/Ca ratio (Fig. S9A) and half for the Ba/Ca ratio (Fig. S9B). It is noteworthy that the samples in the present study come from the same bone powder as those used two decades ago, excluding any problem of contamination that would lead to a consistent offset, which is not the case. The Sr/Ca and Ba/Ca ratios were measured by means of flame and electrothermal atomic absorption spectroscopy (FAAS or ETAAS) in Balter et al. (2002a) and by means of ICPOES or ICPMS in the present study, and in both cases, the accuracy of the Sr/Ca and Ba/Ca of the SRM-1400 CRM was satisfying (Balter et al., 2002a; Supplementary Material; Fig. S2). The only relevant hypothesis to explain the discrepancy between the two sets of measurements is that the stocks of powder samples are not homogeneous and that the bulk value is incorrectly estimated in the present study because we actually collected $\leq$5 mg while about 60 times more (ca. 300 mg) were collected in Balter et al. (2002a). A very low sample amount is necessary when using ICPOES or ICPMS because these techniques are very sensitive, which can explain the generally observed scattering of the bulk trace element results in fossil bone using optical or mass spectrometry.

5.3. Ecological and physiological isotope systematics

The range of δ^{44}Ca values spans ca. 1 ‰ from −2.2 ‰ in the enamel of *Megaloceros* to −1.2 ‰ in the bone of rhinos (Fig. 2A). The overall distribution of the δ^{44}Ca value is consistent with previously published studies, e.g., generally decreasing up the trophic chain (Martin et al., 2018; Hu et al., 2022). This general trend is, however, overprinted by a great deal of variability among herbivores or carnivores and within a given taxon. In the present study, there is a clear distinction between the δ^{44}Ca values of ruminants and those of monogastric herbivores (Fig. 3A; Mann-Whitney test: $p^{***} < 10^{-4}$). This difference is also observed in other studies (Martin et al., 2018; Hu et al., 2022), but taxonomic peculiarities can also be depicted. For instance, the genus *Stegodon*, a ca. 2 Ma elephantid from China, is characterized by very low δ^{44}Ca values

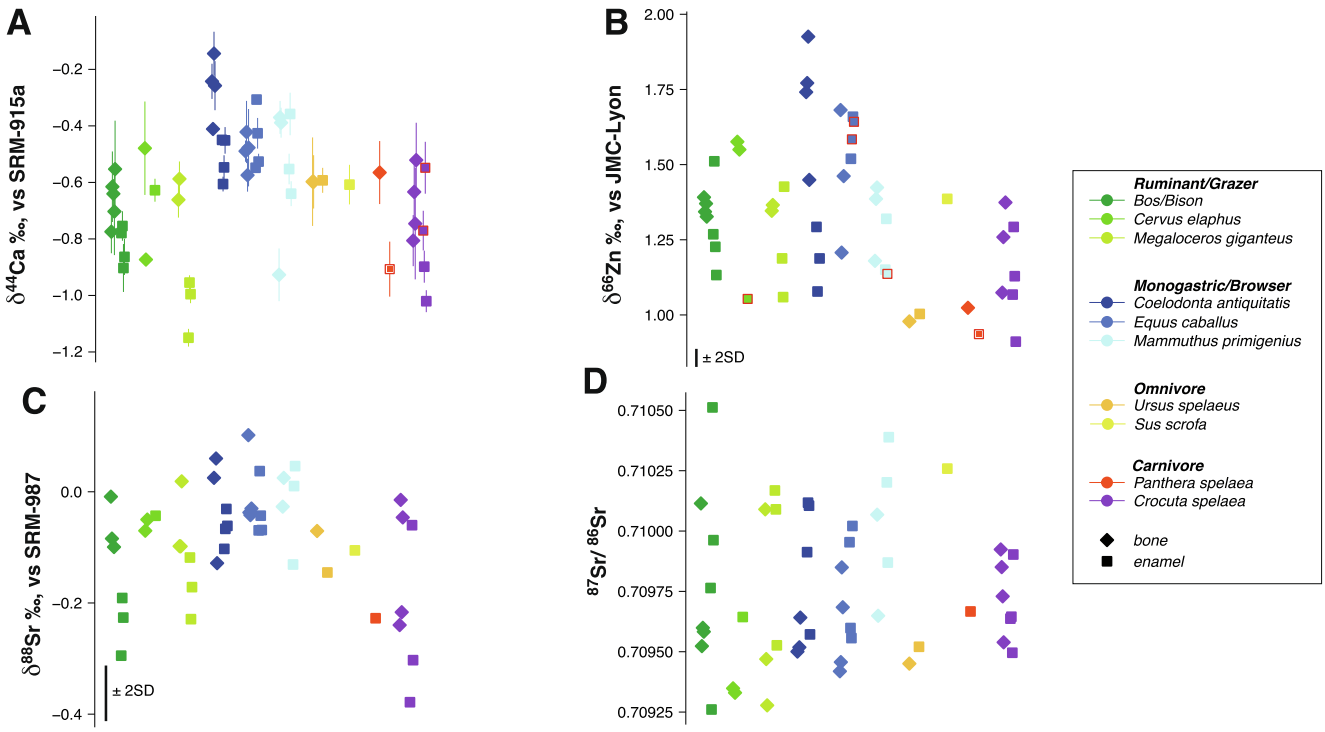

Fig. 2. Taxonomic distribution of bone and enamel isotope compositions. (A) Calcium isotope compositions ($\delta^{44}Ca$). Enamel symbols highlighted with a red stroke have a high Ca/P ratio associated with a high V/Ca ratio (cf Fig. S7). Two-standard deviation of the mean is indicated for each sample. (B) Zinc isotope compositions ($\delta^{66}Zn$). Enamel symbols highlighted with a red stroke have a high Zn/Ca ratio associated with a high Mn/Ca ratio (cf. Fig. S7). A two-standard deviation of the mean is indicated for all samples. (C) Strontium stable isotope compositions ($\delta^{88}Sr$). A two-standard deviation of the mean is indicated for all samples. D) Strontium radiogenic isotope compositions ($^{87}Sr/^{86}Sr$). The symbol size is higher than the two-standard deviation of the mean for all samples.

(Hu et al., 2022), and the actual zebra have significantly lower $\delta^{44}Ca$ values compared to other East-African monogastric herbivores (Martin et al., 2018). These examples clearly demonstrate that the dietary $\delta^{44}Ca$ signature can overcome the prominence of digestive physiology as the main driver of the overall distribution of the $\delta^{44}Ca$ value in mammals. This is especially the case if the so-called group of monogastric herbivores is considered a grazer and the ruminant one a browser, knowing that *Megaloceros* is supposed to be a mixed feeder and the *Bos* genus a heterogeneous feeder (Rivals et al., 2012; Rivals and Lister, 2016; Stefaniak et al., 2020). Clearly, more studies on extant communities are necessary to disentangle the physiological vs. dietary influence on mammals $\delta^{44}Ca$ values. Another aspect of importance is that the Ca isotopic contraction that is usually expected for hyenas due to their bone-crushing diet does not hold at Camiac, where the range of $\delta^{44}Ca$ values encompasses about half of the total variation (Fig. 2A). Does this scattering of the data reflect a diet that is isotopically diverse? Keeping in mind that hyenas preferentially consumed horse, bovine, and rhino (Guadelli, 1989; Discamps, 2011) whose $\delta^{44}Ca$ values span almost 1 ‰, one would expect a resulting heterogeneity in bone or enamel ^{44}Ca values. This hypothesis could be tested in the future by analyzing several aliquots of single hyena specimens. We will show in the last paragraph that the observed variability of the $\delta^{44}Ca$ values is also reflected in other stable isotope compositions and therefore suggests actual dietary variations. The three enamel samples with high Ca/P values associated with elevated V/Ca ratios (Fig. S7C), which therefore have potentially dubious Ca isotope composition, do not exhibit peculiar $\delta^{44}Ca$ values (Fig. 2A).

The range of $\delta^{66}Zn$ values spans ca. 1 ‰ from 1.0 ‰ in the enamel of carnivores to 2.0 ‰ in the bone of rhinos (Fig. 2B). This range of values is comparable to that observed in open-environment trophic chains (Jaouen et al., 2013, 2016a, 2022), i.e., higher than for forested trophic chains (Bourgon et al., 2020, 2021). The clustering according to monogastric/grazer vs. ruminant/browser categories is less relevant for Zn isotopes than for Ca isotopes. The $\delta^{66}Zn$ values (ca. 1 ‰) of *Ursus spelaeus* retain attention. Cave bears are interpreted to be omnivores based on dental microwear (Peigné et al., 2009) or herbivores based on collagen N isotope compositions (Bocherens et al., 1994). Here, the $\delta^{66}Zn$ values of the cave bear specimens exhibit quite low values compared to those of herbivores (Fig. 2B), which could indicate an omnivore or a browser diet, and their mid-range $\delta^{44}Ca$ values (Fig. 2A) suggest that bones of prey were not consumed. The combined use of Ca and Zn isotope ratios therefore supports the herbivory of this individual, possibly of a browsing type. Regarding carnivores, the cave lion exhibits expectedly low $\delta^{66}Zn$ values, while hyenas are characterized by scattered $\delta^{66}Zn$ values encompassing about half of the local variation (Fig. 2B). The consumption of a variable amount of bone has been suggested to explain this pattern (Jaouen et al., 2016a; Bourgon et al., 2021). The apparent contradiction with the $\delta^{44}Ca$ results is discussed further.

The range of $\delta^{88}Sr$ values spans ca. 0.5 ‰ from −0.4 ‰ in the enamel of hyena to 0.1 ‰ in the bone of horse (Fig. 2C). In Guiserix et al. (2022), ruminant herbivores displayed slightly lower $\delta^{88}Sr$ values than carnivores, which is consistent with the pattern observed at Camiac. Overall, the distribution of the $\delta^{88}Sr$ values at Camiac mimics that of the $\delta^{44}Ca$ values (Fig. 2A). The $^{87}Sr/^{86}Sr$ values range from 0.70925 to 0.71050 in the enamel of the genus *Bos* (Fig. 2D). The range of variation is smaller for hyenas compared to any other taxa, suggesting a restricted chasing area around the den, which is characterized by a local $^{87}Sr/^{86}Sr$ value of ca. 0.710 (Willmes et al., 2018).

5.4. Ontogenic isotope systematics

Isotopic values were measured in bone and enamel aliquots from different animal specimens and, as such, cannot be pairwise compared. We therefore computed an average isotopic value for bone and enamel for a given taxon. As a rule, the stable isotope compositions are always

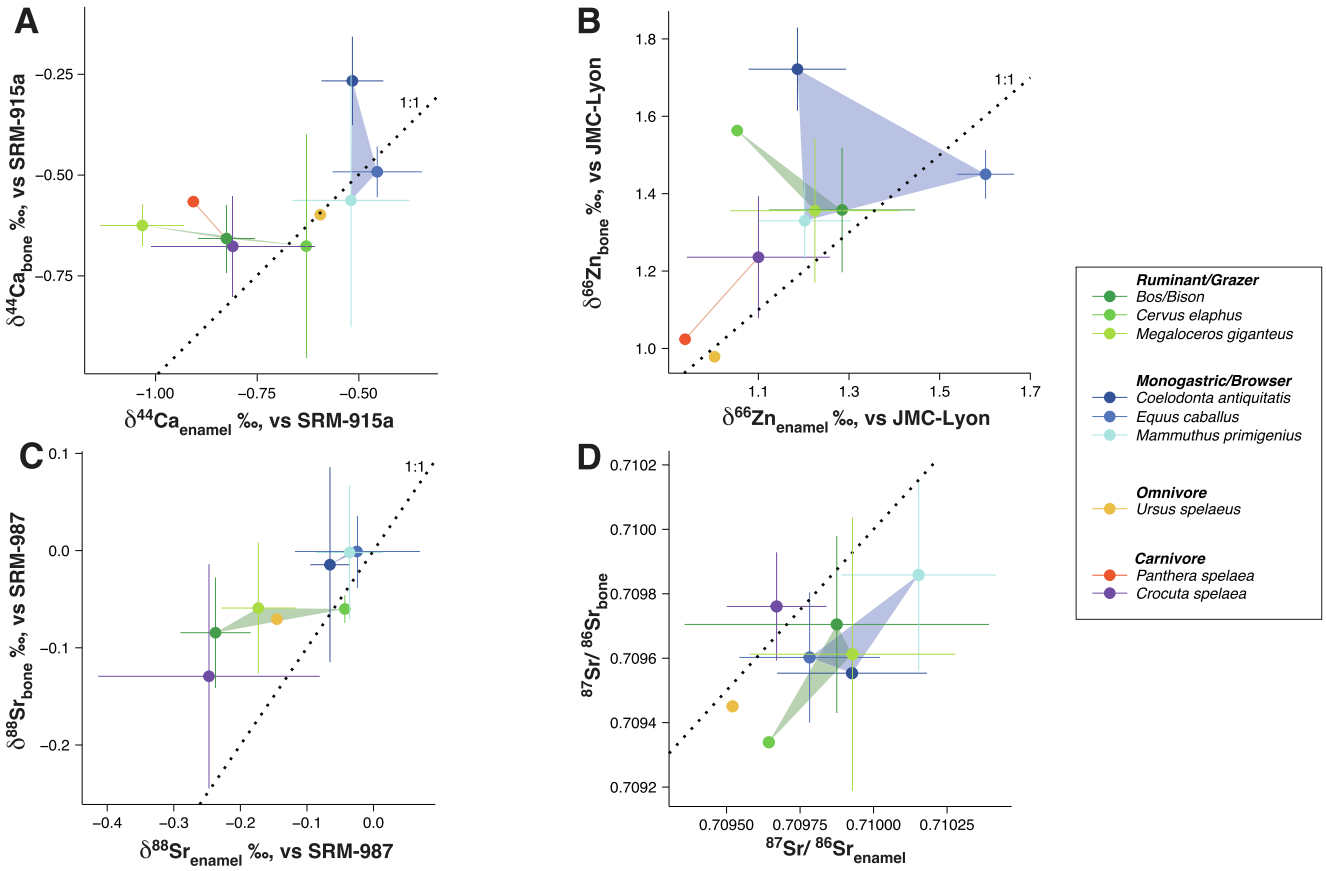

Fig. 3. Correlation of bone vs. enamel averaged isotope compositions as a function of the taxon. Convex hulls are given for ruminant/grazer, monogastric/browser, omnivore, and carnivore groups. A two-standard deviation of the mean is indicated for each taxon. (A) Calcium isotope compositions ($\delta^{44}Ca$). (B) Zinc isotope compositions ($\delta^{66}Zn$). (C) Strontium stable isotope compositions ($\delta^{88}Sr$). (D) Strontium radiogenic isotope compositions ($^{87}Sr/^{86}Sr$).

equal or higher in bone than in enamel (Fig. 3A–C), while it is the opposite for radiogenic Sr, except for hyenas and cave bears, for which the $^{87}Sr/^{86}Sr$ ratios in bone and enamel can be considered similar (Fig. 3D). This suggests that the stable isotope compositions are under distinct crystal-chemical controls in bone and enamel or that an ontogenically-associated dietary effect, such as weaning, differentially affects bone and enamel.

The $\delta^{44}Ca$ values are significantly higher in bone than in enamel (Mann-Whitney, $p^{**} = 0.0017$; Fig. 3A). This is now well explained by a suckling effect (Chu et al., 2006; Li et al., 2016, 2022; Tacail et al., 2017, 2019) with the consumption of milk with a very depleted $\delta^{44}Ca$ value until weaning. A recent study conducted on single specimens shows that the $\delta^{44}Ca$ values of enamel in deciduous teeth and first permanent molars are always lower than in third molars and bone (Hassler et al., 2021). While the difference in the $\delta^{44}Ca$ value between bone and enamel is statistically significant for most of the taxa, there are exceptions, such as for hyenas and horses, for which bone and enamel $\delta^{44}Ca$ values are identical. These peculiarities remain to be elucidated, notably by sampling different tooth types from taxa with different ages at weaning.

The $\delta^{66}Zn$ values are significantly higher in bone (1.34 ± 0.47 ‰, ±2 SD) than in enamel (1.20 ± 0.39 ‰, ±2 SD; Mann-Whitney, $p^{**} = 0.0045$; Fig. 3B) as previously documented by Jaouen et al. (2016a,b), Jaouen and Pons (2017), McCormack et al. (2022). The $\delta^{66}Zn$ offset between bone and enamel can be large, i.e., ca. −0.5 ‰ as in the case of rhinos (Fig. 3B). A suckling effect along with the sampling of different tooth types from taxa with different ages at weaning can explain, as for Ca isotopes, the various observed $\delta^{66}Zn$ offsets observed between bone and enamel if exceeding 0.2 ‰.

The $\delta^{88}Sr$ values are significantly higher in bone than in enamel (Mann-Whitney, $p^{**} = 0.0041$; Fig. 3C). As Sr undergoes a generalized Ca-biopurification in mammals (Balter, 2004), it is not surprising that the patterning of the $\delta^{88}Sr$ values in bone and enamel mimics that of Ca isotopes and that a suckling effect is also efficient for Sr isotopes. Interestingly, Sr radiogenic isotopes display the inverse pattern of Sr stable isotopes, i.e., enamel has significantly higher $^{87}Sr/^{86}Sr$ ratios than bone (Mann-Whitney, $p^{**} = 0.0024$; Fig. 3D). This indicates that all taxa, except hyenas and cave bears, grew up in an area with a higher $^{87}Sr/^{86}Sr$ ratio than Camiac. The similar bone and enamel $^{87}Sr/^{86}Sr$ ratios (Fig. 3D) suggest that hyenas and possibly cave bears chased prey around Camiac since birth and never migrated.

A general scheme is thus emerging in which milk is depleted in heavy isotopes, at least for Ca, Zn, and Sr. To test this hypothesis, we calculated the average isotopic offset between bone and enamel ($\Delta_{bone\text{-}enamel}$) for a given taxon and isotope composition (Fig. S10A and S10B). The results do not show any clear relationship between $\Delta^{44}Ca_{bone\text{-}enamel}$ and $\Delta^{66}Zn_{bone\text{-}enamel}$ values, suggesting that the mechanism that drives the isotopic offset between bone and enamel is not the same for Ca and Zn (Fig. S10A). However, while not significant ($p = 0.093$), the $\Delta^{44}Ca_{bone\text{-}enamel}$ and $\Delta^{88}Sr_{bone\text{-}enamel}$ values seem to be positively correlated (Fig. S10B), indicating that the mechanism at the origin of the Ca isotope fractionation during milk synthesis also fractionates Sr isotopes. These results are not irrelevant since the Sr and Ca metabolisms are linked, but not those of Zn and Ca. The measurement of Ca, Zn, and Sr (among others) isotope compositions in the enamel of different tooth types and in the bone of single mammal specimens would shed light on ontogenic isotope fractionation related to suckling and weaning.

5.5. Ecological and physiological vs. ontogenic isotope systematics

Taken together, the results of the present study show that ecology, physiology, and ontogeny modulate the Ca, Zn, and Sr isotope systematics of mammal hard tissues. We now evaluate their relative influence based on the hypothesis that ecology and/or physiology will drive isotopic patterning preferentially between taxa and ontogeny preferentially between bone and enamel. Generally, ecology and physiology have a stronger influence than ontogeny on stable isotope compositions. A first line of evidence is that for a given isotope composition, the order of magnitude of the $\Delta_{bone\text{-}enamel}$ values (Fig. S10), which should convey ontogeny-related isotope fractionation, is about half that of the total range of variation for bone or enamel (Fig. 3). In other words, the amplitude of the ecological and/or physiological influence is generally similar in bone and enamel, with some exceptions, e.g., *Megaloceros* $^{44}Ca\Delta_{bone\text{-}enamel}$ value (Fig. 2A), rhino $^{66}Zn\Delta_{bone\text{-}enamel}$ value (Fig. 2B), or *Bos* $^{88}Sr\Delta_{bone\text{-}enamel}$ value (Fig. 2C). A second line of evidence is suggested by the absence of overlap between the ruminant/grazer and monogastric/browser groups, both groups being composed by bone and enamel samples ($\delta^{44}Ca$, Mann-Whitney, $p^{***} < 10^{-4}$; Fig. 4A; $\delta^{88}Sr$, Mann-Whitney, $p^{**} = 0.0006$; Fig. 4B). Ecology also exerts an influence on the $\delta^{66}Zn$ values, as suggested by the significant difference between carnivore and herbivore $\delta^{66}Zn$ values (Mann-Whitney, $p^{*} = 0.0392$; Fig. 4A and C).

As mentioned above, we observed significant variability in the studied stable isotope compositions. This is the case, for instance, among hyenas, which can have Ca and Sr isotope compositions in both bone and enamel comparable with herbivores (Fig. 2A and C), or among horses, which exhibit both very positive $\delta^{44}Ca$ and $\delta^{66}Zn$ values (Fig. 2A and B). By comparing the isotope compositions for all bone and enamel samples analyzed in the present study, we show that the stable isotope compositions, but not the radiogenic Sr ratio, are strongly interconnected, which results in significant correlations (Fig. S11). Because it is not possible that diagenesis will be involved for the three isotopic systematics and will be effective for stable, but not radiogenic, Sr isotope compositions, the remaining explanation is that the observed variability actually reflects subtle ecological (e.g., dietary) and/or physiological deviations. Bone and enamel are heterogeneous materials that integrate varying geochemical signals related to complex life histories. Thus, sampling a tiny amount of heterogeneous material increases the variability of the observed geochemical signals. This issue should be resolved by increasing the sample size, however, doing so will go against conservative efforts.

6. Conclusion

The present study has three objectives: (1) the set-up of a protocol to sequentially isolate Ca, Zn, and Sr for stable isotope analyses from a single fossil bone or enamel aliquot, (2) testing the respective preservation of biological Ca, Zn, and Sr concentrations and isotope compositions in bone and enamel, and (3) comparing the patterning of the different isotopic systems in a case study fossil mammal community, Camiac, a hyena den from the upper Pleistocene. The first objective is demonstrated to be achieved by the measurement of accurate concentrations and isotope compositions of Ca, Sr, and Zn in matrix-matched CRMs. Fossil bone is currently less studied than enamel because of its higher susceptibility to diagenesis, however, using an *ad hoc* leaching step and *post-hoc* identification of remaining diagenetic effects, we show

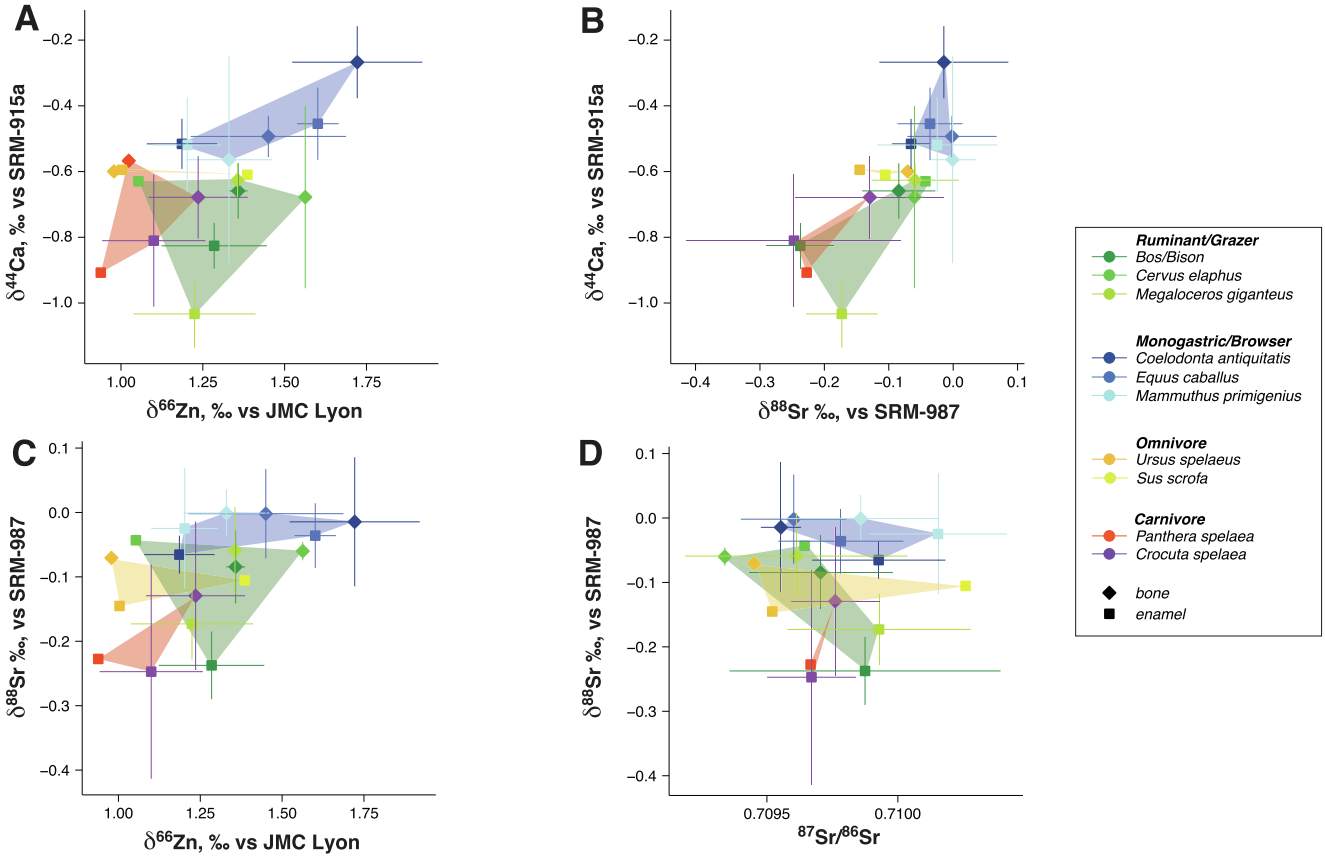

Fig. 4. Correlation between bone and enamel average isotope compositions as a function of the taxon. Convex hulls are given for ruminant/grazer, monogastric/browser, omnivore, and carnivore groups. A two-standard deviation of the mean is indicated for bone and enamel of each taxon. (A) Calcium isotope compositions ($\delta^{44}Ca$) vs. Zn isotope compositions ($\delta^{66}Zn$). (B) Calcium isotope compositions ($\delta^{44}Ca$) vs. Sr isotope compositions ($\delta^{88}Sr$). (C) Strontium stable isotope compositions ($\delta^{88}Sr$) vs. Zn isotope compositions ($\delta^{66}Zn$). (D) Strontium stable isotope compositions ($\delta^{88}Sr$) vs. Sr radiogenic isotope compositions ($^{87}Sr/^{86}Sr$).

through the second objective that fossil bone is potentially a valuable tissue for paleoecological and paleobiological investigations. By tackling the third objective, the results of the present study show that ecology (through diet), physiology, and ontogeny modulate the stable Ca, Zn, and Sr isotope compositions in bone and tooth enamel. Despite the gross interconnection of the three isotopic systems, each has its own patterning. The concomitant study of the three isotopic systems allows for finer paleoecological and paleobiological reconstructions, but more studies are needed to unravel the observed isotopic peculiarities. Focusing on European Paleolithic archaeological sites would be interesting as the paleobiocenoses did not change drastically notwithstanding very changing paleoenvironments. Finally, with the development of new geochemical proxies, such as non-traditional isotopes, it is important to improve sampling protocols to limit the destructive impact on archaeological and paleontological remains. The results obtained during this work open perspectives for the implementation of new sampling protocols that would include the analyses of traditional and non-traditional isotopes in addition to fossil DNA and proteomics on a single aliquot of fossil bone or tooth enamel.

CRediT authorship contribution statement

Jessica Mendes Cardoso: Formal analysis, Writing – review & editing.

Data availability

Data are available through Zenodo at https://doi.org/10.5281/zenodo.8214078.

Declaration of competing interest

The authors declare that they have no known competing financial interests or personal relationships that could have appeared to influence the work reported in this paper.

Acknowledgements

The authors thank Dan Sinclair and two anonymous reviewers for their helpful comments. They also gratefully thank Michel Lenoir for his endless help in gaining access to the fossil remains at Camiac, as well as for the friendly and fruitful discussions. This study was funded by the European Research Council (ERC) Project ARCHEIS (Grant 803676), the CNRS 80| PRIME program and Research Program of the Nouvelle Aquitaine Region: Isotopes du calcium et anthropobiologie au Paléolithique moyen (convention no. 2019-1R40208). Jérôme Schmeleff, Camille Duquenoy, Manuel Henry, and Philippe Télouk are thanked for their help during the study.

Appendix A. Supplementary material

The Supplementary Material to this article contains information on the ion-exchange chemistry for the separation of Ca, Sr, and Zn, mass fractionation of Ca and Zn isotopes, effects of the leaching on the Ca-normalized trace element ratios in fossil and CRM, correlations between concentrations and isotope compositions, and statistical results as heatmaps of correlation coefficients and corresponding significant individual correlations. Supplementary material to this article can be found online at https://doi.org/10.1016/j.gca.2023.12.021.

References

Balter, V., 2004. Allometric constraints on Sr/Ca and Ba/Ca partitioning in terrestrial mammalian trophic chains. Oecologia 139, 83–88.

Balter, V., Bocherens, H., Person, A., Labourdette, N., Renard, M., Vandermeersch, B., 2002a. Ecological and physiological variability of Sr/Ca and Ba/Ca in mammals of West European mid-Würmian food webs. Palaeogeogr. Palaeoclimatol. Palaeoecol. 186, 127–143.

Balter, V., Lamboux, A., Zazzo, A., Télouk, P., Leverrier, Y., Marvel, J., Moloney, A.P., Monahan, F.J., Schmidt, O., Albarède, F., 2013. Contrasting Cu, Fe, and Zn isotopic patterns in organs and body fluids of mice and sheep, with emphasis on cellular fractionation. Metallomics 5, 1470–1482.

Balter, V., Lécuyer, C., 2004. Determination of Sr and Ba partition coefficients between apatite and water from 5°C to 60°C: a potential new thermometer for aquatic paleoenvironments. Geochim. Cosmochim. Acta 68, 423–432.

Balter, V., Person, A., Labourdette, N., Drucker, D., Renard, M., Vandermeersch, B., 2001. Were Neandertalians essentially carnivores? Sr and Ba preliminary results of the mammalian palaeobiocoenosis of Saint-Césaire. Comptes Rendus Académie Sci. – Ser IIA – Earth Planet. Sci. 332, 59–65.

Balter, V., Saliège, J.-F., Bocherens, H., Person, A., 2002b. Evidence of physico–chemical and isotopic modifications in archaeological bones during controlled acid etching. Archaeometry 44, 329–336.

Balter, V., Telouk, P., Reynard, B., Braga, J., Thackeray, F., Albarède, F., 2008. Analysis of coupled Sr/Ca and $^{87}Sr/^{86}Sr$ variations in enamel using laser-ablation tandem quadrupole-multicollector ICPMS. Geochim. Cosmochim. Acta 72, 3980–3990.

Balter, V., Zazzo, A., Moloney, A.P., Moynier, F., Schmidt, O., Monahan, F.J., Albarède, F., 2010. Bodily variability of zinc natural isotope abundances in sheep. Rapid Commun. Mass Spectrom. 24, 605–612.

Bocherens, H., Fizet, M., Mariotti, A., 1994. Diet, physiology and ecology of fossil mammals as inferred from stable carbon and nitrogen isotope biogeochemistry: implications for Pleistocene bears. Palaeogeogr. Palaeoclimatol. Palaeoecol. 107, 213–225.

Bourgon, N., Jaouen, K., Bacon, A.-M., Jochum, K.P., Dufour, E., Duringer, P., Ponche, J.-L., Joannes-Boyau, R., Boesch, Q., Antoine, P.-O., Hullot, M., Weis, U., Schulz-Kornas, E., Trost, M., Fiorillo, D., Demeter, F., Patole-Edoumba, E., Shackelford, L.L., Dunn, T.E., Zachwieja, A., Duangthongchit, S., Sayavonkhamdy, T., Sichanthongtip, P., Sihanam, D., Souksavatdy, V., Hublin, J.-J., Tütken, T., 2020. Zinc isotopes in Late Pleistocene fossil teeth from a Southeast Asian cave setting preserve paleodietary information. Proc. Natl. Acad. Sci. 117, 4675–4681.

Bourgon, N., Jaouen, K., Bacon, A.-M., Dufour, E., McCormack, J., Tran, N.-H., Trost, M., Fiorillo, D., Dunn, T.E., Zanolli, C., Zachwieja, A., Duringer, P., Ponche, J.-L., Boesch, Q., Antoine, P.-O., Westaway, K.E., Joannes-Boyau, R., Suzzoni, E., Frangeul, S., Crozier, F., Aubaile, F., Patole-Edoumba, E., Luangkhoth, T., Souksavatdy, V., Boualaphane, S., Sayavonkhamdy, T., Sichanthongtip, P., Sihanam, D., Demeter, F., Shackelford, L.L., Hublin, J.-J., Tütken, T., 2021. Trophic ecology of a Late Pleistocene early modern human from tropical Southeast Asia inferred from zinc isotopes. J. Hum. Evol. 161, 103075.

Brazier, J.-M., Schmitt, A.-D., Pelt, E., Lemarchand, D., Gangloff, S., Tacail, T., Balter, V., 2019. Determination of radiogenic $^{87}Sr/^{86}Sr$ and stable $\delta^{88/86}Sr_{SRM987}$ isotope values of thirteen mineral, vegetal and animal reference materials by DS-TIMS. Geostand. Geoanalyt. Res.

Budd, P., Montgomery, J., Barreiro, B., Thomas, R.G., 2000. Differential diagenesis of strontium in archaeological human dental tissues. Appl. Geochem. 15, 687–694.

Chu, N.-C., Henderson, G.M., Belshaw, N.S., Hedges, R.E.M., 2006. Establishing the potential of Ca isotopes as proxy for consumption of dairy products. Appl. Geochem. 21, 1656–1667.

Clementz, M.T., Holden, P., Koch, P.L., 2003. Are calcium isotopes a reliable monitor of trophic level in marine settings? Int. J. Osteoarchaeol. 13, 29–36.

DeNiro, M.J., Epstein, S., 1978. Influence of diet on the distribution of carbon isotopes in animals. Geochim. Cosmochim. Acta 42, 495–506.

Deniro, M.J., Epstein, S., 1981. Influence of diet on the distribution of nitrogen isotopes in animals. Geochim. Cosmochim. Acta 45, 341–351.

Discamps, E., Delagnes, E., Lenoir, M., Tournepiche, J.F., 2012. Human and hyena co-occurrences in Pleistocene sites: insights from spatial, faunal and lithic analyses at Camiac and La Chauverie (SW France). J. Taphon. 10, 291–316.

Discamps, E., 2011. La place du Rhinocéros dans le régime alimentaire des hyènes à Camiac (Gironde, France) et ses implications pour la compétition avec les derniers néandertaliens.

Dodat, P.-J., Tacail, T., Albalat, E., Gómez-Olivencia, A., Couture-Veschambre, C., Holliday, T., Madelaine, S., Martin, J.E., Rmoutilova, R., Maureille, B., Balter, V., 2021. Isotopic calcium biogeochemistry of MIS 5 fossil vertebrate bones: application to the study of the dietary reconstruction of Regourdou 1 Neandertal fossil. J. Hum. Evol. 151, 102925.

Dodat, P.-J., Martin, J.E., Olive, S., Hassler, A., Albalat, E., Boisserie, J.-R., Merceron, G., Souron, A., Maureille, B., Balter, V., 2023. Limits of calcium isotopes diagenesis in fossil bone and enamel. Geochim. Cosmochim. Acta 351, 45–50.

Fietzke, J., Liebetrau, V., Günther, D., Gürs, K., Hametner, K., Zumholz, K., Hansteen, T., Eisenhauer, A., 2008. An alternative data acquisition and evaluation strategy for improved isotope ratio precision using LA-MC-ICP-MS applied to stable and radiogenic strontium isotopes in carbonates. J. Anal. At. Spectrom. 23, 955–961.

Guadelli, J.-L., 1989. Etude taphonomique du repaire d'Hyènes de Camiac (Gironde, France). Bull. Assoc. Fr. Pour Létude Quat. 1989–2, 91.

Guiserix, D., Albalat, E., Ueckermann, H., Davechand, P., Iaccheri, L.M., Bybee, G., Badenhorst, S., Balter, V., 2022. Simultaneous analysis of stable and radiogenic strontium isotopes in reference materials, plants and modern tooth enamel. Chem. Geol. 606, 121000.

Hassler, A., Martin, J.E., Amiot, R., Tacail, T., Godet, F.A., Allain, R., Balter, V., 2018. Calcium isotopes offer clues on resource partitioning among Cretaceous predatory dinosaurs. Proc. R. Soc. B Biol. Sci. 285, 20180197.

Hassler, A., Martin, J.E., Ferchaud, S., Grivault, D., Le Goff, S., Albalat, E., Hernandez, J.-A., Tacail, T., Balter, V., 2021. Lactation and gestation controls on calcium isotopic compositions in a mammalian model. Metallomics 13, mfab019.

Heuser, A., Tütken, T., Gussone, N., Galer, S.J.G., 2011. Calcium isotopes in fossil bones and teeth – Diagenetic versus biogenic origin. Geochim. Cosmochim. Acta 75, 3419–3433.
Hu, Y., Jiang, Q., Liu, F., Guo, L., Zhang, Z., Zhao, L., 2022. Calcium isotope ecology of early Gigantopithecus blacki (~2 Ma) in South China. Earth Planet. Sci. Lett. 584, 117522.
Jaouen, K., Pons, M.-L., 2017. Potential of non-traditional isotope studies for bioarcheology. Archeol. Anthropol. Sci. 9, 1389–1404.
Jaouen, K., Pons, M.-L., Balter, V., 2013. Iron, copper and zinc isotopic fractionation up mammal trophic chains. Earth Planet. Sci. Lett. 374, 164–172.
Jaouen, K., Beasley, M., Schoeninger, M., Hublin, J.-J., Richards, M.P., 2016a. Zinc isotope ratios of bones and teeth as new dietary indicators: results from a modern food web (Koobi Fora, Kenya). Sci. Rep. 6, 26281.
Jaouen, K., Szpak, P., Richards, M.P., 2016b. Zinc Isotope Ratios as Indicators of Diet and Trophic Level in Arctic Marine Mammals. PLOS ONE 11, e0152299.
Jaouen, K., Trost, M., Bourgon, N., Colleter, R., Cabec, A.L., Tütken, T., Oliveira, R.E., Pons, M.L., Méjean, P., Steinbrenner, S., Chmeleff, J., Strauss, A., 2020. Zinc isotope variations in archeological human teeth (Lapa do Santo, Brazil) reveal dietary transitions in childhood and no contamination from gloves. PLOS ONE 15, e0232379.
Jaouen, K., Villalba-Mouco, V., Smith, G.M., Trost, M., Leichliter, J., Lüdecke, T., Méjean, P., Mandrou, S., Chmeleff, J., Guiserix, D., Bourgon, N., Blasco, F., Mendes Cardoso, J., Duquenoy, C., Moubtahij, Z., Salazar Garcia, D.C., Richards, M., Tütken, T., Hublin, J.-J., Utrilla, P., Montes, L., 2022. A Neandertal dietary conundrum: Insights provided by tooth enamel Zn isotopes from Gabasa, Spain. Proc. Natl. Acad. Sci. 119, e2109315119.
Knudson, K.J., Williams, H.M., Buikstra, J.E., Tomczak, P.D., Gordon, G.W., Anbar, A.D., 2010. Introducing $\delta^{88/86}$Sr analysis in archaeology: a demonstration of the utility of strontium isotope fractionation in paleodietary studies. J. Archaeol. Sci. 37, 2352–2364.
Koutamanis, D., Roberts, G.L., Dosseto, A., 2021. Inter- and intra-individual variability of calcium and strontium isotopes in modern Tasmanian wombats. Palaeogeogr. Palaeoclimatol. Palaeoecol. 574, 110435.
Lanping, F., Zhou, L., Yang, L., Zhang, W., Wang, Q., Shuoyun, T., Hu, Z., 2018. A rapid and simple single-stage method for Ca separation from geological and biological samples for isotopic analysis by MC-ICP-MS. J. Anal. At. Spectrom. 33, 413–421.
Lazzerini, N., Balter, V., Coulon, A., Tacail, T., Marchina, C., Lemoine, M., Bayarkhuu, N., Turbat, T., Lepetz, S., Zazzo, A., 2021. Monthly mobility inferred from isoscapes and laser ablation strontium isotope ratios in caprine tooth enamel. Sci. Rep. 11, 2277.
le Goff, S., Albalat, E., Dosseto, A., Godin, J.-P., Balter, V., 2021. Determination of magnesium isotopic ratios of biological reference materials via multi-collector inductively coupled plasma mass spectrometry. Rapid Commun. Mass Spectrom. 35, e9074.
Lenoir, M., 2000. La Préhistoire ancienne en Gironde: apport des recherches récentes. Gall. Préhistoire – Archéologie Fr. Préhistorique 42, 57–84.
Lewis, J., Pike, A., Coath, C., Evershed, R., 2017. Strontium concentration, radiogenic (^{87}Sr/^{86}Sr) and stable (δ^{88}Sr) strontium isotope systematics in a controlled feeding study. STAR Sci. Technol. Archaeol. Res. 3, 45–57.
Li, Q., Thirlwall, M., Müller, W., 2016. Ca isotopic analysis of laser-cut microsamples of (bio)apatite without chemical purification. Chem. Geol. 422, 1–12.
Li, Q., Nava, A., Reynard, L.M., Thirlwall, M., Bondioli, L., Müller, W., 2022. Spatially-resolved Ca isotopic and trace element variations in human deciduous teeth record diet and physiological change. Environ. Archaeol. 27, 474–483.
Martin, J.E., Tacail, T., Balter, V., 2017a. Non-traditional isotope perspectives in vertebrate palaeobiology. Palaeontology 60, 485–502.
Martin, J.E., Vincent, P., Tacail, T., Khaldoune, F., Jourani, E., Bardet, N., Balter, V., 2017b. Calcium isotopic evidence for vulnerable marine ecosystem structure prior to the K/Pg extinction. Curr. Biol. 27, 1641–1644.e2.
Martin, J.E., Tacail, T., Cerling, T.E., Balter, V., 2018. Calcium isotopes in enamel of modern and Plio-Pleistocene East African mammals. Earth Planet. Sci. Lett. 503, 227–235.
Martin, J.E., Tacail, T., Braga, J., Cerling, T.E., Balter, V., 2020. Calcium isotopic ecology of Turkana Basin hominins. Nat. Commun. 11, 3587.
McCormack, J., Szpak, P., Bourgon, N., Richards, M., Hyland, C., Méjean, P., Hublin, J.-J., Jaouen, K., 2021. Zinc isotopes from archaeological bones provide reliable trophic level information for marine mammals. Commun. Biol. 4, 1–11.
McCormack, J., Griffiths, M.L., Kim, S.L., Shimada, K., Karnes, M., Maisch, H., Pederzani, S., Bourgon, N., Jaouen, K., Becker, M.A., Jöns, N., Sisma-Ventura, G., Straube, N., Pollerspöck, J., Hublin, J.-J., Eagle, R.A., Tütken, T., 2022. Trophic position of Otodus megalodon and great white sharks through time revealed by zinc isotopes. Nat. Commun. 13, 2980.
Moynier, F., Albarède, F., Herzog, G.F., 2006. Isotopic composition of zinc, copper, and iron in lunar samples. Geochim. Cosmochim. Acta 70, 6103–6117.
Müller, W., Fricke, H., Halliday, A.N., McCulloch, M.T., Wartho, J.-A., 2003. Origin and Migration of the Alpine Iceman. Science 302, 862–866.
Nava, A., Lugli, F., Romandini, M., Badino, F., Evans, D., Helbling, A.H., Oxilia, G., Arrighi, S., Bortolini, E., Delpiano, D., Duches, R., Figus, C., Livraghi, A., Marciani, G., Silvestrini, S., Cipriani, A., Giovanardi, T., Pini, R., Tuniz, C., Bernardini, F., Dori, I., Coppa, A., Cristiani, E., Dean, C., Bondioli, L., Peresani, M., Müller, W., Benazzi, S., 2020. Early life of Neanderthals. Proc. Natl. Acad. Sci. 117, 28719–28726.
Nitzsche, K.N., Wakaki, S., Yamashita, K., Shin, K.-C., Kato, Y., Kamauchi, H., Tayasu, I., 2022. Calcium and strontium stable isotopes reveal similar behaviors of essential Ca and nonessential Sr in stream food webs. Ecosphere 13, e3921.
Peigné, S., Goillot, C., Germonpré, M., Blondel, C., Bignon, O., Merceron, G., 2009. Predormancy omnivory in European cave bears evidenced by a dental microwear analysis of Ursus spelaeus from Goyet, Belgium. Proc. Natl. Acad. Sci. 106, 15390–15393.
Reynard, B., Balter, V., 2014. Trace elements and their isotopes in bones and teeth: Diet, environments, diagenesis, and dating of archeological and paleontological samples. Palaeogeogr. Palaeoclimatol. Palaeoecol. 416, 4–16.
Rivals, F., Lister, A.M., 2016. Dietary flexibility and niche partitioning of large herbivores through the Pleistocene of Britain. Quat. Sci. Rev. 146, 116–133.
Rivals, F., Semprebon, G., Lister, A., 2012. An examination of dietary diversity patterns in Pleistocene proboscideans (Mammuthus, Palaeoloxodon, and Mammut) from Europe and North America as revealed by dental microwear. Quat. Int. 255, 188–195.
Romaniello, S.J., Field, M.P., Smith, H.B., Gordon, G.W., Kim, M.H., Anbar, A.D., 2015. Fully automated chromatographic purification of Sr and Ca for isotopic analysis. J. Anal. At. Spectrom. 30, 1906–1912.
Sillen, A., LeGeros, R., 1991. Solubility profiles of synthetic apatites and of modern and fossil bones. J. Archaeol. Sci. 18, 385–397.
Skulan, J., DePaolo, D.J., 1999. Calcium isotope fractionation between soft and mineralized tissues as a monitor of calcium use in vertebrates. Proc. Natl. Acad. Sci. 96, 13709–13713.
Skulan, J., DePaolo, D.J., Owens, T.L., 1997. Biological control of calcium isotopic abundances in the global calcium cycle. Geochim. Cosmochim. Acta 61, 2505–2510.
Stefaniak, K., Stachowicz-Rybka, R., Borówka, R.K., Hrynowiecka, A., Sobczyk, A., Moskal-del Hoyo, M., Kotowski, A., Nowakowski, D., Krajcarz, M.T., Billia, E.M.E., Persico, D., Burkanova, E.M., Leshchinskiy, S.V., Asperen, E., Ratajczak, U., Shpansky, A.V., Lempart, M., Wach, B., Niska, M., Made, J., Stachowicz, K., Lenarczyk, J., Piątek, J., Kovalchuk, O., 2020. Browsers, grazers or mix-feeders? Study of the diet of extinct Pleistocene Eurasian forest rhinoceros Stephanorhinus kirchbergensis (Jäger, 1839) and woolly rhinoceros Coelodonta antiquitatis (Blumenbach, 1799). Quat. Int.
Tacail, T., Albalat, E., Télouk, P., Balter, V., 2014. A simplified protocol for measurement of Ca isotopes in biological samples. J. Anal. At. Spectrom. 29, 529.
Tacail, T., Télouk, P., Balter, V., 2015. Precise analysis of calcium stable isotope variations in biological apatites using laser ablation MC-ICPMS. J. Anal. At. Spectrom. 31, 152–162.
Tacail, T., Thivichon-Prince, B., Martin, J.E., Charles, C., Viriot, L., Balter, V., 2017. Assessing human weaning practices with calcium isotopes in tooth enamel. Proc. Natl. Acad. Sci. 114, 6268–6273.
Tacail, T., Martin, J.E., Arnaud-Godet, F., Thackeray, J.F., Cerling, T.E., Braga, J., Balter, V., 2019. Calcium isotopic patterns in enamel reflect different nursing behaviors among South African early hominins. Sci. Adv. 5, eaax3250.
Tacail, T., Le Houedec, S., Skulan, J.L., 2020. New frontiers in calcium stable isotope geochemistry: Perspectives in present and past vertebrate biology. Chem. Geol. 537, 119471.
Weber, K., Weber, M., Menneken, M., Kral, A.G., Mertz-Kraus, R., Geisler, T., Vogl, J., Tütken, T., 2021. Diagenetic stability of non-traditional stable isotope systems (Ca, Sr, Mg, Zn) in teeth – An in-vitro alteration experiment of biogenic apatite in isotopically enriched tracer solution. Chem. Geol. 572, 120196.
Willmes, M., Bataille, C.P., James, H.F., Moffat, I., McMorrow, L., Kinsley, L., Armstrong, R.A., Eggins, S., Grün, R., 2018. Mapping of bioavailable strontium isotope ratios in France for archaeological provenance studies. Appl. Geochem. 90, 75–86.
Wooller, M.J., Bataille, C., Druckenmiller, P., Erickson, G.M., Groves, P., Haubenstock, N., Howe, T., Irrgeher, J., Mann, D., Moon, K., Potter, B.A., Prohaska, T., Rasic, J., Reuther, J., Shapiro, B., Spaleta, K.J., Willis, A.D., 2021. Lifetime mobility of an Arctic woolly mammoth. Science 373, 806–808.
Young, E.D., Galy, A., Nagahara, H., 2002. Kinetic and equilibrium mass-dependent isotope fractionation laws in nature and their geochemical and cosmochemical significance. Geochim. Cosmochim. Acta 66, 1095–1104.
Zimmermann, T., Retzmann, A., Schober, M., Proefrock, D., Prohaska, T., Irrgeher, J., 2019. Matrix separation of Sr and Pb for isotopic ratio analysis of Ca-rich samples via an automated simultaneous separation procedure. Spectrochim. Acta B 151, 54–64.